

## Quantum Turbulence in a Propagating Superfluid Vortex Front

V. B. Eltsov,<sup>1,2</sup> A. I. Golov,<sup>3</sup> R. de Graaf,<sup>1</sup> R. Hänninen,<sup>1</sup> M. Krusius,<sup>1</sup> V. S. L'vov,<sup>4</sup> and R. E. Solntsev<sup>1</sup>

<sup>1</sup>Low Temperature Laboratory, Helsinki University of Technology, P.O. Box 5100, 02015 HUT, Finland

<sup>2</sup>Kapitza Institute for Physical Problems, Kosygina 2, 119334 Moscow, Russia

<sup>3</sup>School of Physics and Astronomy, The University of Manchester, Manchester M13 9PL, United Kingdom

<sup>4</sup>Department of Chemical Physics, The Weizmann Institute of Science, Rehovot 76100, Israel

(Received 8 August 2007; published 26 December 2007)

We present experimental, numerical, and theoretical studies of a vortex front propagating into a region of vortex-free flow of rotating superfluid  $^3\text{He-B}$ . We show that the nature of the front changes from laminar through quasiclassical turbulent to quantum turbulent with decreasing temperature. Our experiment provides the first direct measurement of the dissipation rate in turbulent vortex dynamics of  $^3\text{He-B}$  and demonstrates that the dissipation becomes mutual-friction independent with decreasing temperature, and it is strongly suppressed when the Kelvin-wave cascade on vortex lines is predicted to be involved in the turbulent energy transfer to smaller length scales.

DOI: 10.1103/PhysRevLett.99.265301

PACS numbers: 67.57.Fg, 47.32.-y, 67.40.Vs

Turbulent motion of fluids with low viscosity, like water or air, is a general phenomenon in nature and plays an important role in human everyday life. Nevertheless, various features of turbulence are not yet well understood; thus a possibility to study turbulence from another, nonclassical viewpoint looks promising. Flows in superfluids (with zero viscosity) can be turbulent; understanding this form of turbulence is crucial for our ability to describe superfluids, including practical applications like cooling superconducting devices. Turbulence in superfluid  $^4\text{He}$  at relatively high temperatures  $T \sim 1$  K has been studied for decades [1]. Fermi-fluid  $^3\text{He}$  is very different from the Bose-fluid  $^4\text{He}$ ; this allows us to study in  $^3\text{He}$  some aspects of superfluid turbulence not available in  $^4\text{He}$  [2,3].

In this Letter we report the first experimental observation and study of propagating laminar and turbulent vortex fronts in rotating  $^3\text{He}$  which opens a possibility to directly measure the rate of kinetic energy dissipation in a wide temperature range down to  $0.18T_c$  of the critical temperature  $T_c \approx 2.43$  mK (at 29 bar pressure). The idea of the experiment is as follows: in rotating  $^3\text{He}$  (in the  $B$  phase) we can create a vortex-free Landau state, which in the absence of external perturbations persists forever. In this state the superfluid component is at rest in the laboratory frame, while the normal component is in rigid rotation with angular velocity  $\Omega$ . The Landau state is metastable, having larger free energy than the stable equilibrium vortex state. The latter consists of rigidly rotating normal and superfluid components with a regular array of rectilinear quantized vortices. When we inject a seed vortex into the Landau state, we observe a rapid local evolution of the vorticity toward the equilibrium state. A boundary between the vortex free and the vortex states propagates with constant velocity  $V_f$  toward the metastable region(s), see Fig. 1. In some sense this phenomenon is similar to the propagation of a flame front in premixed fuel. The flame front propagation can also proceed in laminar or in turbulent regimes.

In the latter case the effective area of the front increases and its propagation speed becomes higher than in the laminar regime. This property finds its practical use in combustion engines but also has been used to describe intensity curves of type Ia supernovae [4]. In all these cases a metastable state of matter is converted to the stable state in the front and  $V_f$  is determined by the rate of dissipation

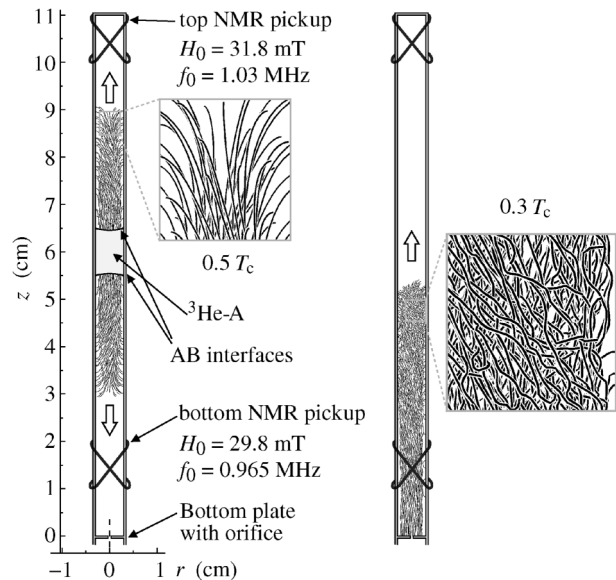


FIG. 1. Experimental setup. (Left) Configuration for vortex injection using  $AB$  interface instability in which two vortex fronts propagate independently in the upper and lower  $B$ -phase sections (as shown by hollow arrows). (Right) Configuration for vortex injection from the orifice when a single vortex front travels first through the bottom and then through the top NMR pickup coils. Superimposed inside the sample container are snapshots of vortex configurations from numerical simulations of vortex expansion at two different temperatures. The configuration at  $0.3T_c$  displays small-scale structure (shown within blowup on the right) which is absent at  $0.5T_c$ .

of the released energy. In our case (with density  $\rho_s$  and velocity  $U = \Omega r$  of the superfluid component in a sample container of radius  $R$ ), the dissipation rate of total kinetic energy,  $\mathcal{E}(t)$ , is related to  $V_f$  as

$$d\mathcal{E}/dt = -\pi\rho_s V_f \Omega^2 R^4/4. \quad (1)$$

Thus by measuring  $V_f$  one determines directly  $d\mathcal{E}/dt$  in turbulent vortex dynamics. So far measurements in the turbulent regime concerned the decay of vortex density, which was found to be temperature independent below  $0.2T_c$  [2].

Our main experimental observation is that  $d\mathcal{E}(t)/dt$  does not go to zero in the  $T \rightarrow 0$  limit. At high enough temperature the front is laminar and its velocity is determined by mutual friction between the normal and superfluid components  $V_f(T) \approx \alpha(T)\Omega R$ , where  $\alpha(T)$  is a dimensionless mutual-friction coefficient. Although  $\alpha(T) \rightarrow 0$  when  $T \rightarrow 0$ , the measured velocity  $V_f(T)$  saturates at a constant value which corresponds to an effective friction  $\alpha_{\text{eff}} \sim 0.1$ . We interpret this behavior to be similar to the *viscous anomaly* in classical turbulence, where the dissipation rate does not vanish when viscosity  $\nu$  goes to zero. The viscous anomaly appears due to cascading of energy to smaller length scales. When  $\nu \rightarrow 0$ , the smallest length scale decreases but the global dissipation rate does not change. We believe that a similar mechanism, which we can call *mutual-friction anomaly*, applies to superfluids where mutual friction plays the role of viscosity. One can say that the viscous and mutual-friction anomalies are particular cases of a more general phenomenon, which we call the *dissipation anomaly*: the nonzero rate of energy dissipation in the limit of a vanishingly small parameter that governs dissipation.

As mutual friction decreases and turbulent motion reaches progressively smaller length scales, eventually quantized vortex lines become important. The energy cascade on length scales smaller than the intervortex distance and the nature of dissipation on such scales are currently the central questions in research on turbulence in superfluids [1]. At the moment only theoretical speculations exist on the role of the nonlinear interaction of Kelvin waves, resulting in a Kelvin-wave cascade [5,6], terminated by quasiparticle emission, and on the role of vortex reconnections which can redistribute energy over a range of scales and also lead to dissipation [7]. Our experiments show evidence for the importance of the Kelvin-wave cascade: we observe a rapid decrease of the front velocity with decreasing temperature in the region where the introduction of sub-intervortex scales to energy transfer is expected. We propose a possible explanation of this effect using a model of crossover between quasiclassical (at super-intervortex scales) and quantum turbulence (at sub-intervortex scales) [8]. A similar drop in dissipation is observed in very recent measurements of turbulent decay in superfluid  $^4\text{He}$  below 0.8 K [9].

*Experiment.*—Our measurements are performed in a rotating nuclear demagnetization cryostat at  $\Omega \sim 1$  rad/s. The  $^3\text{He-B}$  sample at 29 bar pressure is contained in a cylindrical cell with radius  $R = 3$  mm and length 110 mm, oriented parallel to the rotation axis, Fig. 1. Pickup coils of two independent NMR spectrometers near the top and bottom of the cell are used to monitor the vortex configuration [3]. To prepare the initial vortex-free state we heat the sample to about  $0.75T_c$  (for rapid annihilation of all vortices) and then cool it in the vortex-free state in rotation to the target temperature. We can inject seed vortices in the middle of the cell, using the instability of the  $AB$  interface in rotation [3], controlled with an applied magnetic field. In this case two vortex fronts propagate independently up and down, arriving to the top and bottom pickup coils practically simultaneously. A second injection technique uses remanent vortices which are trapped in the vicinity of the orifice on the bottom of the sample, Fig. 1 (right). In this case the vortex front propagates upwards along the entire sample through both pickup coils in succession. We determine the front velocity dividing the flight distance by the flight time, as if the front propagates in steady-state configuration. Although this is not the case due to initial equilibration processes which follow injection, we believe that this simplification is justified here, since the two injection techniques for different propagation lengths give the same result, as seen in Fig. 2.

Our results on the front velocity are presented in Fig. 2. The temperature range is clearly divided in two regions: at  $T \gtrsim 0.4T_c$  the dimensionless front velocity  $v_f = V_f/\Omega R \approx \alpha$ . This agrees with previous measurements in this temperature range and can be understood from the dynamics of a single vortex, when intervortex interactions are ignored [10]. We call this region the laminar regime. The measured values of  $v_f$  are slightly below  $\alpha$ . We believe that the difference is caused by the twisted vortex state [11] behind the front. It reduces the energy difference across the front and correspondingly the front velocity. Estimating the reduction factor from the uniform twist model [11] we get  $v_{f,\text{lam}} = [2/\log(1 + 1/q^2) - 2/q^2]\alpha$ , where  $q = \alpha/(1 - \alpha')$  and  $\alpha'$  is the reactive mutual-friction coefficient. This dependence (the dash-dotted line in Fig. 2) is in good agreement with the experiment.

The new behavior is observed as temperature decreases below  $0.4T_c$ . Here  $V_f$  rapidly deviates to larger values than  $\alpha\Omega R$  and tends to a constant value with a peculiar transition from one plateau to another at around  $0.25T_c$ . We attribute this behavior to turbulent dynamics and analyze it below in more detail.

*Simulations.*—To clarify the vortex front formation and propagation, we simulate vortex dynamics using the vortex filament model with full Biot-Savart equations and an additional solution of the Laplace equation for solid wall boundary conditions [12] in an ideal cylinder with length

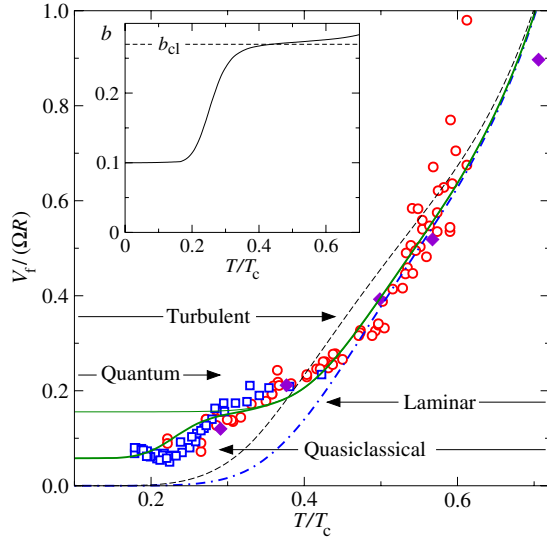


FIG. 2 (color online). Scaled front velocity vs temperature. Open circles and squares mark measurements with injection using  $AB$  interface instability and orifice trapping, respectively, at  $\Omega$  between 0.8 and 1.5 rad/s. Dashed line is the measured value of mutual-friction coefficient  $\alpha(T)$  [19], extrapolated below  $0.35T_c$  with  $\exp(-\Delta/T)$  law [20]. Filled diamonds are results of numerical simulations. Dash-dotted, thin solid, and thick-solid lines show model approximations which sequentially account for dissipation in the large-scale motion, turbulent energy transfer, and bottleneck effect. (Inset) Value of parameter  $b(T)$  in Eq. (4) which was used in producing the thick solid line in the main panel.

40 mm and diameter 3 mm rotating at  $\Omega = 1$  rad/s. In the initial configuration the equilibrium number of vortices is placed close to one end plate of the sample as quarter loops between the end plate and the sidewall of the sample. During evolution, vortices form a front propagating along the sample (for movies, see Ref. [13]). The thickness of the front is  $\Delta(r) \simeq rd$ , where  $d \sim 1$ . For  $T > 0.4T_c$  the front is laminar with smooth vortices that only twist at large scales (Fig. 1, left). For smaller  $T$  the front becomes turbulent demonstrating a lot of small-scale vortex structure: Kelvin waves, kinks, semiloops (Fig. 1, right). These small-scale fluctuations exist on the background of strongly polarized vortex orientation, which is still preserved at low temperatures. The calculated front velocity is in good agreement with the measurements, see Fig. 2. In particular, the velocity is lower than  $\alpha\Omega R$  at higher temperatures and propagation becomes relatively much faster at lower temperatures.

*Analytical model.*—We consider the turbulent front using the quasiclassical “coarse-grained” equation averaged over the vortex lines [3,14],

$$\dot{\mathbf{U}} + (1 - \alpha')(\mathbf{U} \cdot \nabla)\mathbf{U} + \nabla\mu = -\Gamma\mathbf{U}, \quad \Gamma = \alpha\omega_{\text{ef}}. \quad (2)$$

It describes the evolution of the superfluid velocity  $\mathbf{U}(\mathbf{r}, t)$  at scales exceeding the crossover scale  $\ell$  between hydro-

dynamic and kinetic regimes of turbulent motions, which is of the order of the intervortex separation. In Eq. (1)  $\mu$  is the chemical potential and the dissipative term  $\Gamma$  is taken in the simplified form [15], in which  $\omega_{\text{ef}}$  can be understood as an effective vorticity.

To estimate  $V_f$  in the quasiclassical regime, as described by Eq. (1), we consider the total energy dissipation in the front with well-developed turbulence which has two contributions. The first one originates from the mutual friction which acts on the global scale. It can be estimated from Eq. (1) as  $\alpha\omega_{\text{ef}}K(z, r)$ , where  $K(z, r) = \frac{1}{2}\langle u^2 \rangle$  is the turbulent kinetic energy per unit mass and  $u$  is the turbulent velocity fluctuations (with zero mean). The second contribution is determined by the usual energy flux in classical turbulence  $\varepsilon \simeq bK^{3/2}(r)/L(r)$  at an outer scale of turbulence  $L(r)$ . Clearly,  $L(r) \simeq \Delta(r)$ , the thickness of the turbulent front at given radius  $r$  near the center line of the cell, or, near the surface of the cell, as distance to surface,  $R - r$ . In the whole cell, one can use an interpolation formula  $L^{-1}(z) = \Delta(r)^{-1} + (R - r)^{-1}$ . The natural assumption is that this energy dissipates on the way to small scales either due to the mutual friction at moderate temperatures or converts into Kelvin waves at the crossover scale  $\ell(r)$ . For the classical Kolmogorov-41 regime  $b_{\text{cl}} \simeq 0.27$  [16]. Using Eq. (1) we present the overall energy budget:

$$V_f\Omega^2R^4 = 8 \int_0^{R-\ell} r dr dz \left[ \Gamma K(z, r) + \frac{K^{3/2}(z, r)}{L(r)} \right]. \quad (3)$$

Here we accounted for the mutual-friction correction to the nonlinear term in Eq. (1)  $b \Rightarrow (1 - \alpha')$  and used the axial symmetry to perform the integration over the azimuthal angle. The region with  $R - r < \ell$ , where Eq. (1) is not applicable, is excluded from the integration.

In the turbulent boundary layer the kinetic energy is independent of the axial distance to the wall. Therefore, qualitatively we can replace  $K(z, r)$  and  $\omega_{\text{ef}}(z, r)$  by their mean values across the front,  $\bar{K}(r)$  and  $\bar{\omega}_{\text{ef}}(r)$ . Dimensional reasoning dictates  $\Delta(r)\bar{\omega}_{\text{ef}}(r) \simeq a\Omega r$  and  $\bar{K}(r) = c(\Omega r)^2/2$  with  $a, c \sim 1$ . Now Eq. (3) gives:

$$v_f \equiv V_f/\Omega R \simeq (2c)^{3/2}b(1 - \alpha')A + 4ca/5\alpha, \quad (4)$$

where  $A = 0.2 + d[\ln(R/\ell) - 137/60 + 5\ell/R + \dots] \simeq 1.8$  for  $\Omega = 1$  rad/s which gives  $R/\ell \simeq 17$ . We take  $b = b_{\text{cl}}$  and choose the parameters  $a = 0.2$ ,  $c = 0.25$ , and  $d = 2$ , to fit the measurement in the region  $(0.3-0.4)T_c$ . With these parameters Eq. (4) gives  $v_f \simeq 0.16$  in the limit  $T \rightarrow 0$  (when  $\alpha = \alpha' = 0$ ) and a very weak temperature dependence up to  $T \simeq 0.45T_c$ . However, both in the region of lower and higher temperatures the experiment shows deviation from this “plateau” (Fig. 2).

The reason for this deviation at  $T > 0.35T_c$  is that turbulence is not well developed near the cylinder axis where the shear of the mean velocity, responsible for turbulence excitation, decreases. Therefore, in the intermediate temperature region only part of the front volume is turbulent,



expanding toward the axis when the temperature decreases. We suggest an interpolating formula between laminar and turbulent regimes:  $v_f = (v_{f,\text{lam}}^2 + v_{f,\text{turb}}^2)^{1/2}$ , where  $v_{f,\text{turb}}$  is given by Eq. [4]. This interpolation is shown in Fig. 2 as a thin line for  $T < 0.3T_c$  and as a thick line for  $T > 0.3T_c$ . The agreement with our experimental observation for  $T > 0.3T_c$  is good, but there is a clear deviation below  $0.25T_c$ , where  $\alpha \approx 10^{-2}$ . The reason is that we did not account adequately for the quantum character of turbulence, which becomes important in our conditions at  $T < 0.3T_c$  [17], which is close to the measured transition to the lower plateau in Fig. 2.

The mean free path of  $^3\text{He}$  quasiparticles at  $T \approx 0.3T_c$  is close to  $\ell$  while at  $0.2T_c$  it exceeds  $R$ . This change from the hydrodynamic to the ballistic regime in the normal component may influence the mutual-friction force acting on the individual vortices. We neglect this effect because for  $T < 0.3T_c$  the mutual friction is already very small and does not directly affect  $V_f$ . In addition, at these temperatures the superfluid remains closely coupled to the external frame of reference: even at  $0.2T_c$  the response in the flow field (as observed with NMR) is delayed with respect to the change in rotation velocity by less than 2 s.

One possibility for the peculiar decrease of dissipation at about  $0.25T_c$  is the following: at these temperatures the energy flux toward small scales propagates to the quantum scale  $\ell$  and vortex discreteness and quantization effects become most important. Even though some part of the energy is lost in intermittent vortex reconnections, the dominant part proceeds to cascade below the scale  $\ell$  by means of nonlinearly interacting Kelvin waves [1,5–7]. The Kelvin waves are much less efficient in the downscale energy transfer than classical hydrodynamic turbulence which may lead to a bottleneck accumulation of the kinetic energy at crossover scale up to  $\Lambda^{10/3}$  times with respect to its K41 value [8]. In our experiments  $\Lambda \equiv \ln(\ell/a_0) \approx 10$  ( $a_0$  is vortex-core radius) and the inertial interval  $R/\ell$  is about one decade. Therefore, the distortion of the energy spectrum due to the bottleneck can reach the outer scale, which leads to a suppression of the energy flux at given turbulent energy, i.e., to a decrease in the effective parameter  $b$ , which relates  $\varepsilon$  and  $K$ . The mutual-friction damping removes some energy from the cascade and thus decreases the bottleneck effect. We checked the temperature dependence  $b(T)$  using the stationary energy balance equation for the energy spectrum  $E_k$  in  $\mathbf{k}$  space,

$$\frac{d\varepsilon(k)}{dk} = -\Gamma(T)E_k,$$

$$\varepsilon(k) \equiv -(1 - \alpha') \sqrt{k^{11} E_k} \frac{d(E_k/k^2)}{8dk},$$

in which  $\Gamma(T)$  is the damping (2), and the energy flux over scales  $\varepsilon(k)$  is taken in the Leih differential approximation [18]. In the calculations we use  $L/\ell = 12$  as ratio of the

outer and crossover scales and characterize the bottleneck with the boundary condition  $E_k/[k^3 d(E_k/k^2)/dk] = -4 \times 10^5$  at the crossover scale. The resulting function  $b(T)$ , shown in the inset in Fig. 2, decreases from its classical value  $b_{\text{cl}}$  down to  $\approx 0.1$  for  $T < 0.2T_c$  in a steplike manner. Inserting the calculated  $b(T)$  in Eq. (4), we get the temperature dependence of the quantum-turbulent front shown in Fig. 2 by the thick solid green line, which is in reasonable agreement with our experimental data. The significant decrease of the dissipation rate in the quantum regime is a consequence of the relative proximity of the outer and quantum crossover scales in our measurement.

*Conclusions.*—The conversion of metastable vortex-free rotating  $^3\text{He-B}$  to stable state occurs via propagation of a dynamic vortex structure, a vortex front, whose nature depends on the magnitude of mutual-friction dissipation. At temperatures below  $0.45T_c$  sustained turbulence appears in the front, profoundly affecting the vortex dynamics. Owing to the energy transfer in the turbulent cascade, dissipation becomes temperature and mutual friction independent at the lowest temperatures. In this regime we have observed the influence of a quantum cascade, involving individual vortices, on the global dissipation rate.

This work is supported by ULTI-4 (No. RITA-CT-2003-505313), Academy of Finland (Grants No. 211507 and No. 114887), and the US-Israel Binational Science Foundation.

- 
- [1] W. F. Vinen and J. J. Niemela, *J. Low Temp. Phys.* **128**, 167 (2002).
  - [2] D. I. Bradley *et al.*, *Phys. Rev. Lett.* **96**, 035301 (2006).
  - [3] A. P. Finne *et al.*, *Rep. Prog. Phys.* **69**, 3157 (2006).
  - [4] S. I. Blinnikov *et al.*, *Astron. Astrophys.* **453**, 229 (2006).
  - [5] E. V. Kozik and B. V. Svistunov, *Phys. Rev. Lett.* **92**, 035301 (2004).
  - [6] W. F. Vinen, *Phys. Rev. B* **61**, 1410 (2000); W. F. Vinen *et al.*, *Phys. Rev. Lett.* **91**, 135301 (2003).
  - [7] B. V. Svistunov, *Phys. Rev. B* **52**, 3647 (1995); E. Kozik and B. Svistunov, arXiv:cond-mat/0703047.
  - [8] V. S. L'vov *et al.*, *Phys. Rev. B* **76**, 024520 (2007).
  - [9] P. M. Walmsley *et al.*, arXiv:0710.1033 [*Phys. Rev. Lett.* (to be published)].
  - [10] A. P. Finne *et al.*, *J. Low Temp. Phys.* **134**, 375 (2004).
  - [11] V. B. Eltsov *et al.*, *Phys. Rev. Lett.* **96**, 215302 (2006).
  - [12] R. Hänninen *et al.*, *J. Low Temp. Phys.* **138**, 589 (2005).
  - [13] R. Hänninen, <http://ltd.tkk.fi/~rhannine/front>.
  - [14] E. B. Sonin, *Rev. Mod. Phys.* **59**, 87 (1987).
  - [15] V. S. L'vov *et al.*, *JETP Lett.* **80**, 535 (2004).
  - [16] V. S. L'vov *et al.*, *JETP Lett.* **84**, 62 (2006).
  - [17] G. E. Volovik, *JETP Lett.* **78**, 533 (2003).
  - [18] C. Leith, *Phys. Fluids* **10**, 1409 (1967).
  - [19] T. D. C. Bevan *et al.*, *Phys. Rev. Lett.* **74**, 750 (1995).
  - [20] I. A. Todoshchenko *et al.*, *J. Low Temp. Phys.* **126**, 1449 (2002); we used the superfluid gap  $\Delta = 1.968T_c$ .